








Corrosion resistance of 5052 aluminum alloy using hydrophobic silane coatings

Daiana Guerra Sacilotto¹ , Sandra Raquel Kunst² , Luana Góes Soares² , Carlos Leonardo Pandolfo Carone² 
Daiana Cristina Metz Arnold² , Claudia Trindade Oliveira² , Jane Zoppas Ferreira² 

¹Universidade Federal do Rio Grande do Sul, Programa de Pós-Graduação em Engenharia de Minas, Metalúrgica e de Materiais, Laboratório de Corrosão. Av. Bento Gonçalves, 9500, Campus do Vale, Agronomia, Porto Alegre, RS, Brasil.

²Universidade Feevale, Instituto de Ciências Criativas e Tecnológicas. RS 239, 2755, Vila Nova, 93352-000, Novo Hamburgo, RS, Brasil.

e-mail: daianasacilotto@gmail.com, tessaro.sandra@gmail.com, lugo.es.soares@gmail.com, carlos.carone@gmail.com, daim@feevale.br, cto@feevale.br, jane.zoppas@ufrgs.br

ABSTRACT

The fabrication of silane-based hydrophobic surfaces depends on factors such as organic substitution reactions, the extension of the surface area being covered, and the distribution of hydroxyl groups on the surface area to increase the anchoring of the coating and consequently improve the corrosion resistance of the metal. In this sense, the objective of the present work is to evaluate the corrosion resistance of the 5052 aluminum alloy was evaluated by the development of hydrophobic surfaces using silanes. Nanoparticles (NPTs) of tetraethoxysilane silane (TEOS) were used to provide morphological roughness for the studied substrates. TEOS and vinyltriethoxysilane (VTES) NPTs were combined to verify the synergistic effect occurring when obtaining angles greater than 150°. The fabrication of the TEOS NPT solution was based on propanone and sodium hydroxide, whereas for the mixing of the VTES solution, ethanol, water and acetic acid were used. The silane deposition was carried out using dip coating and electro-assisted techniques. The aluminum substrate with the silane coatings was tested using two variations of surface morphology, as-received (L) and blasted (J). Substrate composition was verified by X-ray fluorescence (XRF). Contact angle (CA) analysis was performed to evaluate the hydrophobicity provided by the coating. The morphology of the substrates was analyzed by TEM (transmission electron microscopy). Corrosion resistance was verified by electrochemical impedance spectroscopy (EIS) and potentiodynamic polarization. The results obtained from the VTES coating tests verified that a potential of -1.2 V, combined with the blasted substrate, provided lower wettability. However, the results of the electrochemical tests showed that smooth surfaces with film deposition and potentials of -1.2 V and -0.8 V had more corrosion resistance compared to the other analyzed samples.

Keywords: Aluminum alloy; Corrosion; Coating; Hydrophobic silanes.

1. INTRODUCTION

The high applicability of aluminum and its alloys in several sectors of society, such as the aerospace, transport, civil and maritime fields, makes it one of the main metals currently used. The abundant application of this substrate is due to its efficient characteristics, notably its low density, excellent machinability, high fatigue resistance, excellent heat conduction and low cost. However, when aluminum is in contact with ions dissolved in water – especially halides (in particular Cl⁻) –, they can attack its natural oxide layer, destroying the passivity of this material at localized points. In the resulting active-passive cell, the anodic area is in regions where the passive layer is destroyed, which become small in relation to the cathodic areas and thus accelerate the corrosion process at these points [1, 2]. In this context, aiming to increase the durability of this metal in environments prone to triggering corrosive processes, hydrophobic silane coatings have become a promising alternative (insert references, take one from materials research on hydrophobic silanes).

Silanes offer excellent corrosion protection and adhesion properties when used to create organic coatings and can also serve as coupling agents. These properties come from the ability that silanes have to form bonds with both inorganic and organic surfaces, as they have an inorganic and an organic part in their molecular

structure, thus being defined as hybrid compounds. Their organic groups have properties of polymeric materials, increasing the flexibility and functional characteristics of coatings. In turn, their inorganic groups have properties of ceramic materials, which increase the resistance, durability and adhesion to the metallic substrate of coatings [3].

Generally, for the production of hydrophobic silanes, aliphatic hydrocarbons and non-polar fluorinated hydrocarbons are used as the main substituents, which allow the silane molecule to induce the hydrophobicity of the coating. It is known that most substrates that require the application of coatings are polar; that is, they are easily wetted by water. However, the application of hydrophobic films circumvents this polarity of the substrate, making it impermeable. During the deposition of the film on the substrate, the hydroxyls in the silane molecule are adsorbed to the substrate. In the presence of hydroxyls, described here as residual groups that remain after the condensation process, they become “sites” of water adsorption. Thus, for the fabrication of a “successful” hydrophobic coating, hydroxyls (hydrogen bonds) must be eliminated, and the polar substrate, protected from any interaction with water by a non-polar interface [4]. In this sense, the objective of the present study was to obtain hydrophobic silane coatings in order to improve the corrosion resistance of 5052 aluminum alloys.

2. EXPERIMENTAL PROCEDURES

2.1. Materials

AA5052 aluminum plates measuring 7×4 cm were used as substrates and a chemical composition of the AA5052 alloy is illustrated in Figure 1.

The coatings analyzed were from alkoxide precursors, as follows: TEOS (98% – Aldrich Chemistry) + VTES (96% – Aldrich Chemistry) NPT coatings were obtained; a second sample was manufactured from a 50% mixture of each solution, which had a single coating curing phase and was named in the IST results. On the other hand, to produce the samples using the electro-assisted deposition of TEOS NPTs, the respective potentials for the application of the VTES layer were followed.

2.2. Surface preparation of samples

The initial stage of surface preparation is based on the process of obtaining roughness. To avoid the contamination of the particles used in the blasting process and of the metal surface itself, first, the samples were washed using commercial detergent and water. Roughness was developed by two methods detailed below: Sandblasting: for the sandblasting process, a Renfert sandblasting unit with $50 \mu\text{m}$ alumina microparticles was used. This method is carried out manually; i.e., the control of the distance and angle of emission of the microparticles on the substrate is performed manually, since the emitter tip of these comes from a mobile and malleable polymeric tube. This process was chosen because it is a simple, cheap and scalable method that can be applied to parts with more complex structures. TEOS nanoparticles: Tetraethoxysilane nanoparticles (TEOS NPTs) were developed

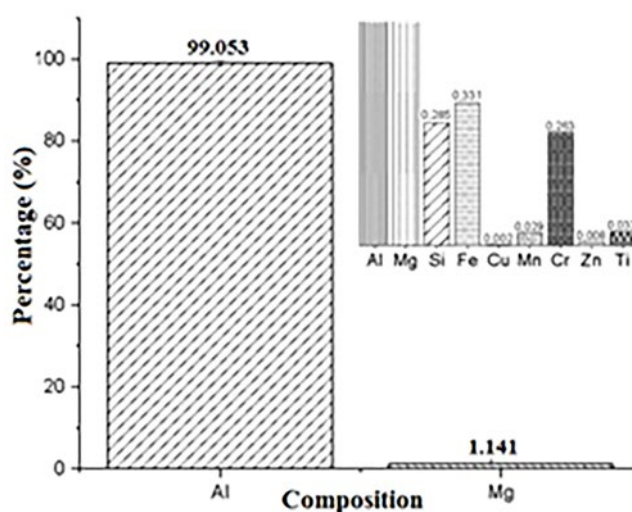


Figure 1: Graph of the X-Ray fluorescence analysis of aluminum alloy 5052 containing the percentage of elements Al, Mg, Si, Fe, Cu, Mn, Cr, Zn and Ti.

synthetically in order to homogenize the surface roughness of the substrate. Their synthesis was based on the use of Propanone P.A 99% from Synth, 0.1 mol/L sodium hydroxide and TEOS in proportions of 93:3:4% by volume, respectively. The deposition of NPTs was performed after the surface degreasing step. Unlike sanding and blasting processes, which change the roughness of the metallic substrate itself, the deposition of nanoparticles produces a “rough” coating layer. Thus, this process was carried out after degreasing, in order to obtain high adhesion to the metallic surface. Electro-assisted deposition was used to deposit TEOS TPNs, applying a potential of -0.8 V for 3 minutes using an Autolab PGSTAT 302 potentiostat from Ecochemie. A transparent acrylic cell was built to this end, where the working electrode was adjusted in the middle of two counter electrodes of AISI 304 steel, with the presence of a Ag/AgCl reference electrode. The sample drying/curing process took place at 125 °C for 60 minutes.

2.3. Degreasing and surface activation

The degreasing of the samples was carried out in a Saloclean commercial alkaline solution. This step aimed to remove organic contaminants as well as oils and dirt on the metallic surface and, simultaneously, perform surface activation due to the adhesion of hydroxyl groups ($-OH$) to the surface. The degreasing process, simultaneously with the activation process, consisted of immersing the substrate for 5 minutes in a preheated solution at $65-70$ °C [5]. Afterward, the samples were washed in running water to remove excess degreaser, then washed with deionized water and dried with a jet of hot air. The time span of 5 minutes was chosen for the aluminum alloy due to its high reactivity (amphoteric character) in alkaline solution, despite the use of a specific degreaser for aluminum. The degreasing efficiency was verified by the water break test. The depositions of the silane-based coating were carried out in the subsequent step.

2.4. Preparation of solutions, deposition and curing of the silane coating

The vinyltriethoxysilane solution was prepared using VTES, deionized water and ethanol (99.5% P.A. – Synth) in the proportions of 6%/47%/47% by volume, respectively. The pH of the solution was adjusted with acetic acid (100% P.A. – Synth), 1 mol/L, to pH 4 [6]. The reagents were mixed using electromagnetic stirring for 2 h at room temperature. The samples were deposited by dip coating for 3 minutes and cured at 150 °C for 60 minutes in an oven. The surface free energy of the substrate coated with TEOS NPTs was altered with the deposition of the VTES solution using the same electro-assisted deposition parameters for TEOS. This phase involved applying a potential of -0.8 V to the material for 3 minutes using the Autolab PGSTAT 302 potentiostat from Ecochemie, with subsequent curing in an oven at 150° for 60 minutes. In both procedures, each sample was produced in triplicate in order to verify the reproducibility of the results. A “new” solution of the respective coating was used for each sample. After drying/curing, the samples were stored in a desiccator.

Coating combinations were performed in order to increase hydrophobicity and corrosion resistance. The results of transmission electron microscopy, CA and EIS using a double layer of silane based on nanoparticles of tetraethoxysilane (TEOS NPTs) and vinyltriethoxysilane (VTES) will be presented. Both coatings were applied by electro-assisted deposition with potentials of -0.8 , -1.2 and -1.6 V.

2.5. Nomenclature of samples

Table 1 presents the list of acronyms comprising the nomenclature of the samples used in this study, where they are divided in relation to substrate, roughness and coating. A representative nomenclature scheme for the studied samples was adopted in Table 1, where L/B = smooth AA5052 aluminum sample as received from the supplier

Table 1: Acronyms used in the nomenclature of the samples.

ACRONYMS	NAME
<i>Substrate</i>	
Al	Aluminum
<i>Substrate</i>	
S	Straight (as received from the supplier company)
S	Sandblasted
TEOS NPTs	Tetraethoxysilane nanoparticles
<i>Coating applied</i>	
VTES	Vinyltriethoxysilane
B	Blank (no coating)

company without coating (white); J/B = uncoated sandblasted AA5052 Aluminum sample (white); L/VTES-0.8V = Aluminum sample AA5052 smooth as received from the company with vinyltriethoxysilane silane and TEOS NPTs deposition applying potential of -0.8 V; L/VTES-1.2V = Aluminum sample AA5052 smooth as received from the company with silane vinyltriethoxysilane and TEOS NPTs deposition applying potential of -1.2 V. J/VTES-0.8V = Aluminum sample AA5052 sandblasted with silane vinyltriethoxysilane and deposition of TEOS NPTs applying potential of -0.8 V; J/VTES-1.2V = AA5052 aluminum sample blasted with vinyltriethoxysilane silane and TEOS NPTs deposition applying potential of -1.2 V.

2.6. Characterization of samples

2.6.1. X-ray fluorescence

X-ray fluorescence (FRX) analysis was performed to assess the chemical composition of the substrate used in this work. This technique allows identifying chemical elements that have an atomic number greater than 10 ($Z > 10$), establishing their existing proportion in the sample. To carry out this non-destructive and qualitative analysis, a Thermo Scientific handheld FRX analyzer – model Niton XL3T – was used. Figure 1 shows the X-Ray fluorescence analysis of the 5052 aluminum alloy, indicating that the 5052 aluminum alloy has a high degree of purity in its composition, being 99% (± 0.551) aluminum, 1% magnesium and containing other chemical elements in smaller proportion, such as Si (0.285%), Fe (0.331%), Cu (0.002%), Mn (0.029%), Cr (0.263%), Zn (0.008%) and Ti (0.033%). According to the composition presented in Figure 1, it is observed that the alloy 5052 Al presents good plasticity, moldability, corrosion resistance and weldability.

The results obtained through FRX analysis were compared with the nominal composition of AA5052 aluminum. To this end, the following chemical composition presented by Silva *et al.* was used as a basis: Si (0.5%), Fe (0.23%), Cu (0.002%), Mn (0.058%), Mg (2.324%), Cr (0.176%), Zn (0.003%) and Ti (0.013%) [7]. The chemical components found in this study (Figure 1) were similar to this composition. Previously, in the study by ALIASGHARI *et al.*, [8] the following proportions were also mentioned for 5052 aluminum: Si $< 0.25\%$, Fe $< 0.4\%$, Cu $< 0.1\%$, Mn 0.15–0.35 %, Mg 2.2–2.8%, Cr $< 0.1\%$, and the presence of zinc and titanium was not detected.

2.6.2. Transmission electron microscopy

The size of the TEOS NPTs was characterized using a Jeol JEM 1200 ExII transmission electron microscope.

2.6.3. Contact angle

3 μ L drops of distilled water were deposited using a Krüss Drop Shape Analyzer – as 30 – and a Phoenix Mini P10001 contact angle analyzer. The results presented below were obtained using the calculated mean of the contact angle (CA) of 5 drops from each specimen of the triplicate, via the Surftens 4.5 software.

2.6.4. Electrochemical tests

For both tests, an Autolab PGSTAT 302 potentiostat from Ecochemie and a conventional three-electrode cell were used, with a saturated Ag/AgCl reference electrode and a platinum counter-electrode. All assays, for each sample, were performed in triplicate. For all measurements, 0.1 mol/L NaCl solutions (pH 6.0) were used, with the exposure of an area of 1.0 cm² of the working electrode. The potentials shown in the results are described in relation to the potential of the reference electrode used. A Faraday cage was used to avoid external interference in the signal. EIS analyses were performed under open circuit potential (OCP) after 30 minutes of immersion in the 0.1 mol/L NaCl solution for system stabilization. The sinusoidal signal used was 10 mV, and the frequency range varied from 104 to 10⁻² Hz, at room temperature. The test used a 1 mV/s sweep. The samples were monitored from 0 to 96 hours (being analyzed each 24 hours until completing the 96 hour cycle) of immersion in the NaCl electrolyte using the FRA software, 0 hour being after the 30 minutes of stabilization under open circuit potential (OCP). The potentiodynamic polarization test was carried out after 5 minutes under OCP to stabilize the potential of the samples after immersion in the solution. The sweep range (from the cathodic area to the anodic area) was from -0.400 V to $+0.500$ V, with a sweep speed of 1 mV.s⁻¹. Corrosion tests were performed in triplicate.

3. RESULTS AND DISCUSSIONS

3.1. Electrochemical impedance spectroscopy

Figure 2 shows the Bode phase diagrams plots obtained after 2 hours of immersion in 0.1 M NaCl comparing samples L/B = Aluminum sample AA5052 smooth as received from the supplier company without coating (white); J/B = uncoated sandblasted AA5052 Aluminum sample (white); L/VTES-0.8V = Aluminum sample

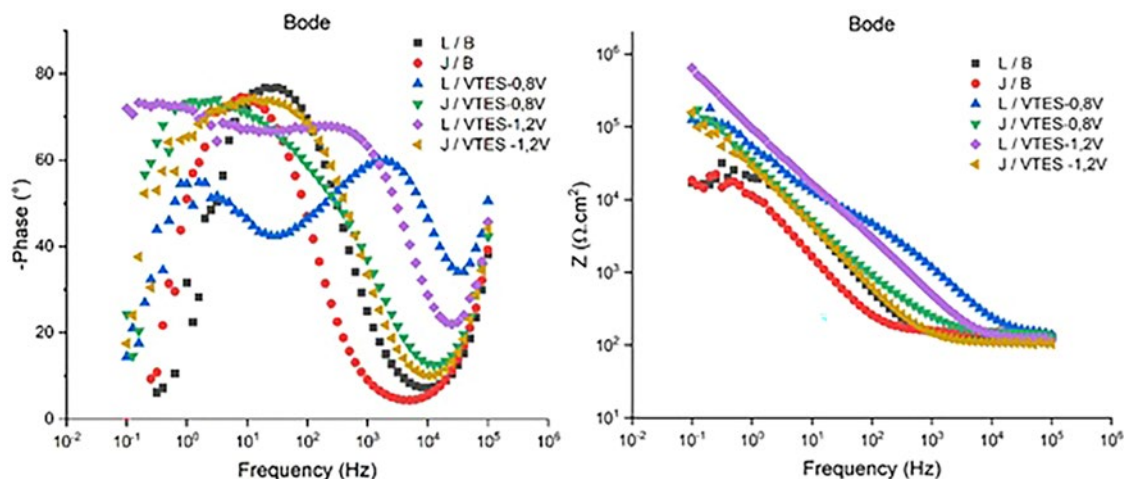


Figure 2: Bode phase diagrams plots obtained after 2 hours of immersion in 0.1 M NaCl comparing samples L/B, J/B, L/VTES-0.8V, L/VTES-1.2V, J/VTES-0.8V, J/VTES-1.2V.

AA5052 smooth as received from the company with vinyltriethoxysilane silane and TEOS NPTs deposition applying potential of -0.8 V; L/VTES-1.2V = Aluminum sample AA5052 smooth as received from the company with silane vinyltriethoxysilane and TEOS NPTs deposition applying potential of -1.2 V. J/VTES-0.8V = Aluminum sample AA5052 sandblasted with silane vinyltriethoxysilane and deposition of TEOS NPTs applying potential of -0.8 V; J/VTES-1.2V = AA5052 aluminum sample blasted with vinyltriethoxysilane silane and TEOS NPTs deposition applying potential of -1.2 V.

After 2 hours of immersion, a phenomenon is observed at high frequency and another at medium and low frequency with a high phase angle value (of around 72°). After 24 hours of immersion, this low-frequency phenomenon disappears, but a “broad” medium frequency phenomenon with a high phase angle appears, and the high-frequency phenomenon remains, with a small shift toward lower frequencies and a small decrease in its phase angle. This high-frequency phenomenon is associated with the silane barrier film, which denotes a resistance to charge transfer. The corrosion protection mechanism of films based on alkoxy-silanes is relatively simple, as it does not involve electrochemical protection; i.e., protection occurs through a physical barrier. The good barrier properties of the coatings are due to the development of a dense Si-O-Si network, which results in the formation of a compact, uniform and adherent film on the substrate. This film retards corrosion, preventing the passage of ions from the medium to the metallic substrate, making it difficult for aggressive species to penetrate [9]. Furthermore, the adhesion of the silane film to a thicker barrier oxide layer, which is naturally formed on aluminum in contact with air, possibly made the oxides more stable, enabling a greater resistance to corrosion. After 48 hours of immersion and until the end of the test at 96 hours, the high-frequency phenomenon disappeared and only a well-defined phenomenon appeared at medium frequency. The latter was associated with the permeability of the electrolyte through the film, yet a high phase angle value (of around 70°) indicates that permeation may have occurred, albeit at a slower pace. CÂNDIDO *et al.* [10] also verified this type of behavior in aluminum silane films, associating it with the passive oxide growth on the surface. However, they add that this passivation is not enough to guarantee adequate resistance. Figure 3 shows the Bode phase diagrams plots obtained during times of 2, 24, 48, 72 and 96 hours of immersion in 0.1 M NaCl for the AA5052 aluminum sample sandblasted with silane vinyltriethoxysilane and deposition of TEOS TPNs applying -1.2 V potential.

At all immersion times (2, 24, 48, 72 and 96 hours), a well-defined phenomenon was observed at medium frequency with a high phase angle value (72°). This phenomenon appears similarly in the uncoated samples and in the sandblasted sample with VTES coating applied at a potential of -0.8 V, indicating that the silane film did not show good adhesion to the sandblasted substrate and that the resistance found at medium frequency is associated with the aluminum oxide. This medium-frequency behavior was also reported by RIBEIRO *et al.* [11], who associated it with the change in electrical conductivity of the passive oxide formed on the surface during exposure to a corrosive environment, possibly related to the charge-transfer effect. To ensure that sandblasted samples have better corrosion resistance properties, in addition to studying other mechanisms to improve the adhesion of the coating to the substrate, it is important to control the distance and angle of incidence of the alumina microparticles during the blasting process, aiming at greater homogeneity of the surface roughness obtained. These parameters must be monitored, since the angle of the microparticle, when colliding with the

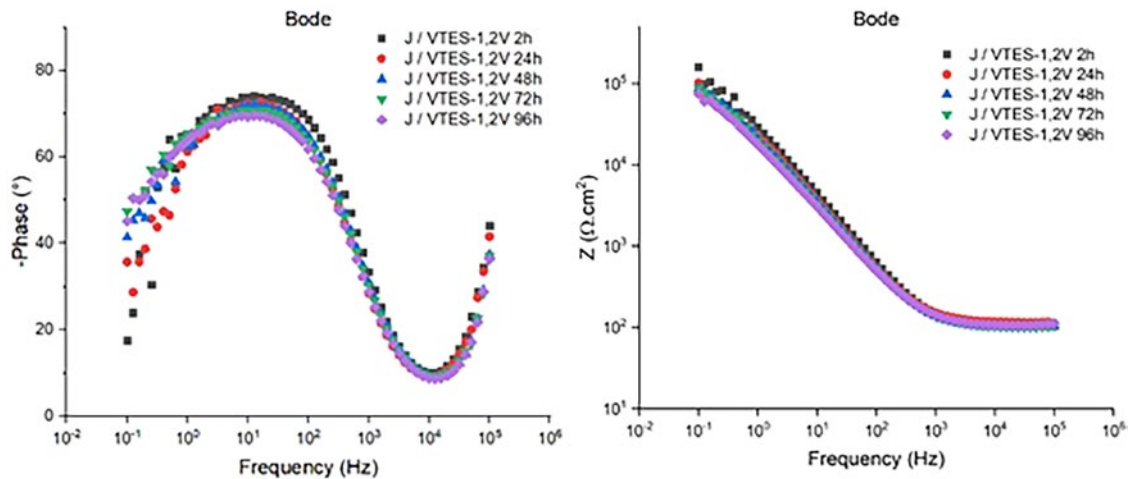


Figure 3: Bode phase diagrams plots obtained during the times of 2, 24, 48, 72 and 96 hours of immersion in NaCl 0.1 M for the sample of Aluminum sample AA5052 sandblasted with silane vinyltriethoxysilane and deposition of TEOS NPTs applying potential of -1.2 V.

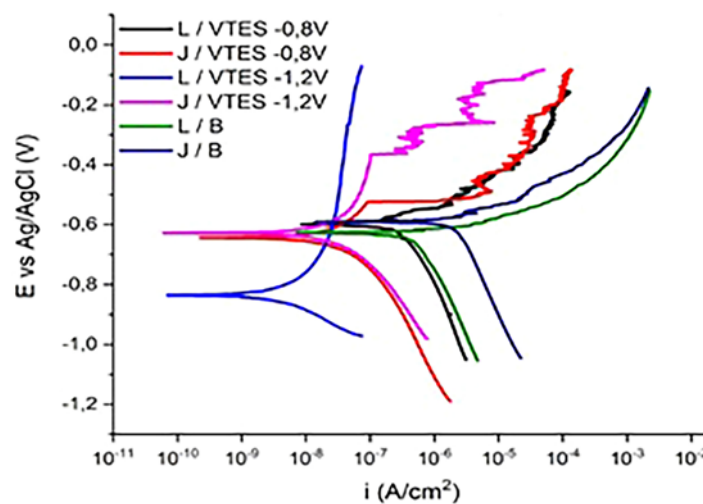


Figure 4: Potentiodynamic polarization curves of samples L/B, J/B, L/VTES-0.8V, L/VTES-1.2V, J/VTES-0.8V, J/VTES-1.2V in NaCl 0 solution 1 mol/L.

substrate, determines the inclination and direction of the peak, while the distance (peak to peak) is related to the height of the formed peak. When considering peak height, it is important to remember that the relationship of a peak to its neighboring peaks can determine the degree of wettability, as droplets can become trapped between their valleys due to the difference in height and distance.

3.2. Potentiodynamic polarization

The graph in Figure 4 presents the potentiodynamic polarization curves in 0.1 M NaCl for the samples Samples L/B = Aluminum sample AA5052 smooth as received from the supplier company without coating (white); J/B = uncoated sandblasted AA5052 Aluminum sample (white); L/VTES-0.8V = Aluminum sample AA5052 smooth as received from the company with vinyltriethoxysilane silane and TEOS NPTs deposition applying potential of -0.8 V; L/VTES-1.2V = Aluminum sample AA5052 smooth as received from the company with silane vinyltriethoxysilane and TEOS NPTs deposition applying potential of -1.2 V. J/VTES-0.8V = Aluminum sample AA5052 sandblasted with silane vinyltriethoxysilane and deposition of TEOS NPTs applying potential of -0.8 V; J/VTES-1.2V = AA5052 aluminum sample blasted with silane vinyltriethoxysilane and deposition

Table 2: Simulation of the Tafel lines of the studied samples (L/B, J/B, L/VTES-0.8V, L/VTES-1.2V, J/VTES-0.8V, J/VTES-1.2V).

SAMPLES	ICORR (A/cm ²)	ECORR (V)
L/VTES -0.8 V	4.05×10^{-7}	-0.588
J/VTES -0.8 V	2.10×10^{-8}	-0.644
L/VTES -1.2 V	3.82×10^{-9}	-0.835
J/VTES -1.2 V	1.12×10^{-8}	-0.628
L/B	4.53×10^{-7}	-0.635
J/B	1.37×10^{-6}	-0.588

of TEOS NPTs applying a potential of -1.2 V. Table 2 shows the extrapolation of the taffel lines from the polarization curves of the Figure 4.

Comparing the uncoated samples (L/B and J/B), the smooth sample showed better electrochemical performance, with a corrosion current density an order of magnitude lower than the sandblasted sample (Table 2), demonstrating that the Al_2O_3 layer plays an important role in substrate protection. This indicates that the blasting process significantly affects the structure of the metallic surface, making it more vulnerable to corrosive processes. Analyzing the polarization curves of the samples with coatings, it can be noted that the L/VTES -1.2 V sample has a lower corrosion current density (Table 2), an order of magnitude in relation to the sandblasted samples, two orders of magnitude in relation to the L/VTES -0.8 V sample and three orders of magnitude in relation to the smooth uncoated aluminum sample. This result corroborates the EIA data, in which this sample was the only one that had a high frequency phenomenon after 2 and 24 hours of immersion associated with the silane barrier film, denoting resistance to charge transfer (Figure 2). In addition, this result demonstrates that although aluminum has a natural resistance conferred by the aluminum oxide, this is adsorbed by Cl^- . The literature reports several types of mechanisms for the attack of Cl^- anions on the aluminum oxide film: via the transport of chloride ions through the oxide film by oxygen vacancies [12], transport of chloride ions through the oxide film by conductive pathways, and localized dissolution of the film and thinning of the oxide layer [13].

The coated samples J/VTES -0.8 V, L/VTES -1.2 V and J/VTES -1.2 V showed corrosion current densities at least one order of magnitude lower in relation to the aluminum sample without coating (Table 2), which highlights the importance of silane coatings in anticorrosive protection. The group led by Van Ooij has extensively studied silane-based treatments of the AA 2024-T3 Al alloy. They have carried out investigations with the objective of obtaining more protective silane films, involving varied conditions for preparing the silane solution, using mixtures of different types of silanes [14] and silanes containing different functional groups in their structure. Their results proved that the silanes inhibit the corrosion of the AA 2024-T3 Al alloy. The L/VTES -0.8 V sample shows similar behavior to the L/B sample, with corrosion current density of the same order of magnitude, as well as similar potentials (Table 2). This result is in accordance with the Bode phase diagrams plots shown in Figure 2, where, for 2 hours of immersion, a phenomenon on average at low frequency and a phase angle of approximately 50° were observed, being reported as a controlled diffusion of the corrosive process occurring at the metal/coating interface. TAMBORIM *et al.* [14] also observed in the silane-based coating on the AA 2024-T3 aluminum alloy two time constants in the first hour of immersion, in low-frequency region. The time constants were attributed by the authors to inductive processes being characterized by diffusion due to the presence of pores in the silane layer. It can be seen that in the case of these samples (sandblasted), with the VTES film being obtained at both -0.8 V and -1.2 V, they have a well-defined pitting potential (approximately -0.5 and -0.4 V, respectively), which can be explained by heterogeneous deposition due to surface irregularity. Analyzing the potentials used for the application of the coating, it can be concluded that the -1.2 V potential yields better results when compared to -0.8 V. The variation of potentials when performing the coating deposition had the goal of analyzing the influence of potentials on the fabrication of a coating with better corrosion resistance properties.

3.3. CHARACTERIZATIONS OF ALUMINUM - TEOS + VTES

3.3.1. Transmission electron microscopy

Figure 5 shows the micrographs obtained by Transmission Electron Microscopy of tetraethoxysilane nanoparticles (TEOS NPTs) produced using a solution of propanone, TEOS and sodium hydroxide. To analyze the influence of the proportion of NaOH added in the manufacturing process, using the pH variation of the solution as a parameter, varying the pH between 8, 10 and 12.

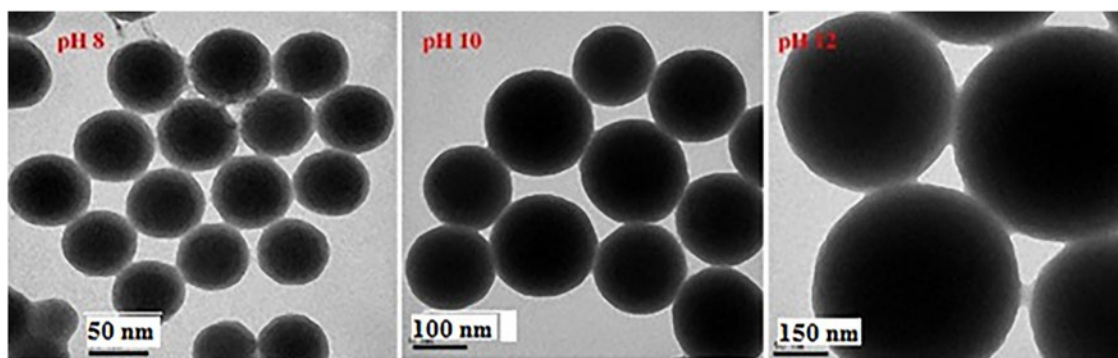


Figure 5: Micrographs obtained by Transmission Electron Microscopy of tetraethoxysilane nanoparticles (TEOS NPTs) produced using propanone solution, TEOS and sodium hydroxide, influence of pH variation of the solution in values between 8, 10 and 12.

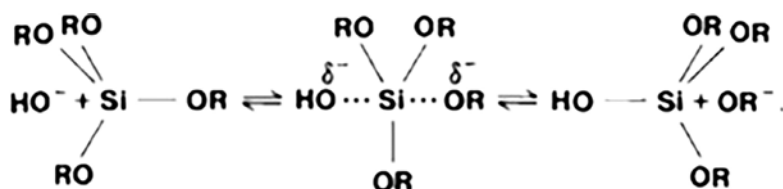


Figure 6: Mechanism of hydrolysis reaction in a basic medium [21].

According to Figure 5, regardless of the pH value, the TPNs were connected in a network, showing several agglomerates deposited on top of the plate used for analysis under the microscope, which is satisfactory for the subsequent adhesion of the silane layer. It is documented in the literature that the hydrolysis of silanes and the condensation of silanol groups are accelerated in alkaline media [15, 16]. According to the literature regarding different metals, one of the most important aspects for the stability and good performance of silane layers is the formation of metal-siloxane bonds (Me-O-Si) with the metallic substrate [17]. For this to occur satisfactorily, the presence of a large number of hydroxyl groups on the surface of the metal is necessary, which is favored by a deposition in alkaline solution [18]. Aluminum is highly sensitive to alkali attack [19], so it is expected that after caustic attack, only a thin layer of oxide will cover the electrode surface. According to TEO *et al.* [18], during silane treatment, aluminum is simultaneously subjected to attack, protonation and coupling reactions. These processes must be favored by the presence of fine oxides (naturally formed), which explains the better performance in terms of adhesion, coverage and, consequently, corrosion resistance when the samples show alkaline behavior [20]. The hydrolysis reaction has a mechanism that is highly dependent on the type of catalyst employed, since silicon alkoxides have low reactivity. In an alkaline medium, water quickly dissociates to produce nucleophilic hydroxyl anions in a first stage. The hydroxyl anion, in turn, attacks the silicon atom inverting the tetrahedron [21]. Figure 6 shows the hydrolysis reaction mechanism in alkaline medium.

Given this behavior, the alkaline attack tends to increase the concentration of hydroxyls on the metal surface, making it more active, which favors the formation of metallic hydroxides (Me-OH) [22]. The greater formation of metallic hydroxides promotes an increase in the amount of metalloxane bonds (Me-O-Si) on the surface, improving the adhesion efficiency of the organosilane layers on the metal. Studies show that alkaline treatments with sodium hydroxide applied to metals, in addition to increasing the concentration of hydroxyls on their surface, promotes the removal of surface impurities [22]. Hence, it can be stated that the increase in the pH of the solution (which becomes more alkaline) has an influence on the increase in size of the nanoparticles. At pH 8, particles with an average size of 50 nm are verified in the solution; at pH 10, they increase to 100 nm and grow to 150 nm in diameter with a pH of 12. When the reactions are catalyzed by a base, a rapid gelation occurs, as evidenced by the turbidity in the solution, which indicates the presence of condensation products. Conversely, when reactions are catalyzed by acid, due to hydrolysis being favored, a slow gelation is observed [23]. In view of this, the pH of the mixture must be adjusted to a certain value, in which the maximum hydrolysis rate of

the alkoxy-silanes molecules and the minimum condensation rate of the already-hydrolyzed alkoxide molecules (silanol) in the solution are achieved to obtain a coating [23]. In this case, the formation of TEOS NPTs was aimed at the homogeneous generation of roughness to be deposited on the substrate. In view of this goal, despite having obtained higher mean values in terms of particle size with the increase in pH, we opted for the lowest pH value (pH 8). This is due to the identification, during the analysis, of a greater tangle of particles united in a single network, which creates, analogically, a more homogeneous coating on the surface. Therefore, in this study, the samples manufactured with TEOS NPTs are 50 nm in diameter; that is, with a pH 8 solution.

3.3.2. Contact angle

The hydrophobicity of a surface is entirely linked with the surface energy of a solid, and can be evaluated by the CA formed by a drop of liquid in relation to the surface. In this phenomenon, the greater the surface free energy, the greater the wettability and, consequently, the greater the adhesion of liquids. Greater adhesion of liquids results in a smaller contact angle, which indicates a more hydrophilic character of the surface [19]. Given this behavior, the degree of hydrophobicity that a surface coating promotes is directly related to its anti-corrosion protection capacity, which is proportional to the CA between the liquid and the coating surface. Figure 7 shows the values with the images obtained from the contact angle for all coated samples: Aluminum sample AA5052 smooth as received from the company with vinyltriethoxysilane silane and TEOS NPTs deposition applying different potentials: -0.8 V, -1.2 V and -1.6 V and AA5052 Aluminum sample sandblasted with silane vinyltriethoxysilane and deposition of TEOS NPTs applying different potentials: -0.8 V, 1.2 V and 1.6 V. And Table 3 presents a comparison of samples with smooth and sandblasted surfaces in relation to the type of coating (NPTs + VTES or VTES) and applied potential for coating deposition (-0.8 V, -1.2 V and -1.6 V).

In Figure 7, it is possible to visualize that the largest contact angles are formed by the sandblasted samples, showing, on average, 40° of greater hydrophobicity in relation to the samples with a smooth surface. The verification of the contact angle, under the same electro-assisted deposition conditions used only for VTES, serves to confirm or disagree with the results obtained previously. Additionally, the verification is done to analyze the influence of adding TEOS NPTs (pH 8) as the first layer/roughness of the deposited coating, considering that the CA of samples L/B (39.1°) and L/J (26.7°) remained the same due to their lack of coatings. In Figure 7, only the results for samples coated with TEOS + VTES are shown. Coatings based on alkoxy silanes, when well cross-linked, have an extremely hydrophobic character. Authors report that in this case, the film is able to reduce the permeability of electrolytes, promoting an effective barrier protection [24].

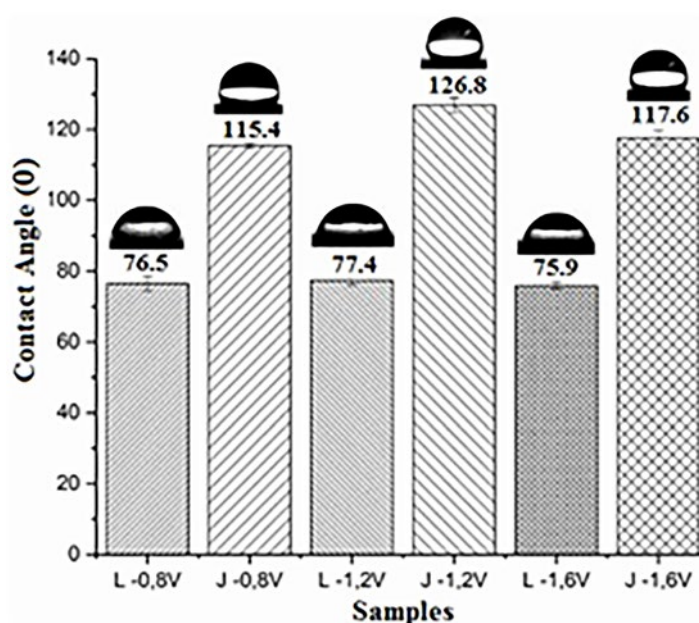


Figure 7: Graph of the values with the images obtained from the contact angle for all coated samples: AA5052 aluminum sample smooth as received from the company with vinyltriethoxysilane silane and TEOS NPTs deposition applying different potentials: -0.8 V, -1.2 V and -1.6 V and AA5052 Aluminum sample sandblasted with silane vinyltriethoxysilane and deposition of TEOS NPTs applying different potentials: -0.8 V, 1.2 V and 1.6 V.

Table 3: CA comparison of samples with smooth and sandblasted surfaces in relation to the type of coating (NPTs + VTES or VTES) and applied potential for coating deposition (−0.8 V, −1.2 V and −1.6 V).

CA (°)						
Potential	−0.8 V		−1.2 V		−1.6 V	
Surface	L	J	L	J	L	J
VTES	83.6	110.2	71.1	118.7	71.0	93.5
NPTs + VTES	76.5	115.4	77.4	126.8	75.9	117.6

However, according to the same authors, the CA of a properly-cross-linked silane-based film is approximately 90°, attesting to a high hydrophobicity in all sandblasted samples, as they showed values higher than 90°, which demonstrates that the adhesion increased with the removal of oxides. In addition, this higher hydrophobicity indicates an improvement in the barrier protection of the alloy, which decreases the permeation of electrolytes, as well as the leaching of chloride ions on the silane layer corroding the metal. This result may be related to an increase in anchorage provided by the sandblasting process to the organosilane coating, due to a better chemical interaction. The literature describes satisfactory results for the application of sandblasting with alkaline solutions, in the case of coatings based on alkoxy-silane precursors, since the presence of hydroxyl groups on the surface is desirable for this coating, so that the metallosiloxane bond (Me-O-Si) occurs [16].

Samples with a smooth surface had contact angles smaller than 80°, a value that underscores the importance of the roughness development process to achieve the hydrophobicity of a material. Furthermore, the roughness of the TEOS NPTs, deposited together with the VTES coating, did not contribute to the increase in the CA of these samples. It is noteworthy that the silane-based coating may show instability in its Si-O-Si groups, and, eventually, they undergo hydrolysis reactions when in contact with an aqueous solution, forming hydrophilic Si-OH groups again [24–26]. This instability is related to the pre-treatment of the surface and the lack of adhesion on the aluminum oxide. VAN OOIJ and ZHU [27] demonstrated that organosilane coatings failed due to the delamination resulting from the formation of cathodic hydroxyl groups at the aluminum interface. Many authors have shown that surface pre-treatment is the most important step for the good performance of a coating system. These authors demonstrated that, without the surface pre-treatment step, the coating delaminates from the surface much more quickly when exposed to aggressive aqueous environments. When observing the CA of the samples, it can be noted that there was a general increase in hydrophobicity; i.e., the presence of TEOS provided an increase in the contact angle. A double layer of silane gives the coating a lower probability of failure and greater thickness. Therefore, it appears that the contact angles of the samples coated with TEOS + VTES NPTs have increased hydrophobicity compared to the coating with only VTES, as shown in Table 3.

Studies performed by VAN OOIJ and ZHU *et al.* [27] showed that a silane monolayer is not sufficient to provide the metallic substrate with good protection against corrosion. Therefore, it is recommended that the metals be covered with a bilayer, two-step treatment. The first layer grants corrosion protection and adhesion to the metallic substrate, while the function of the second layer is to react with the organosilane layer so as to provide good adhesion to the metal/coating system. The second layer is formed by the reaction between the Si-OH groups of each layer, resulting in a siloxane network at the interface. Thus, the two-layer treatment forms a barrier that is more effective and hydrophobic, and, consequently, with greater anti-corrosion performance. RAHIMI *et al.* [22] developed a multilayer coating using the dip coating method by applying the precursors tetraethoxysilane silane (TEOS) and 3-glycidioxypropyltrimethoxysilane (GPTMS) to the AA5083 alloy. The hybrid films were produced by the dip coating technique with exposure to the sun for 2 minutes and a removal and entry speed of 2 cm.min^{−1}. After the application of the coating, the samples were dried at 60 °C for 1 hour. The influence of the double and triple layer was investigated; however, in the last layer the hybrid film was cured at 130 °C for 1 hour. The authors concluded that the hybrid film obtained by the triple layer had the best performance in the electrochemical tests. The morphological results showed hybrid films (double and triple layer) without cracks and with homogeneous distribution on the substrate, in addition to no significant alterations regarding wear resistance.

3.3.3. Electrochemical impedance spectroscopy

Due to the great instability of the electrochemical system, the Bode phase diagrams plots in this section only display data obtained after 24 hours of analysis. The results at 2 hours are similar, but the data have several random points when analyzed at low frequencies. In this study, only the curves of the samples with the application of the −1.2 V potential were plotted, considering that these samples showed greater hydrophobicity in

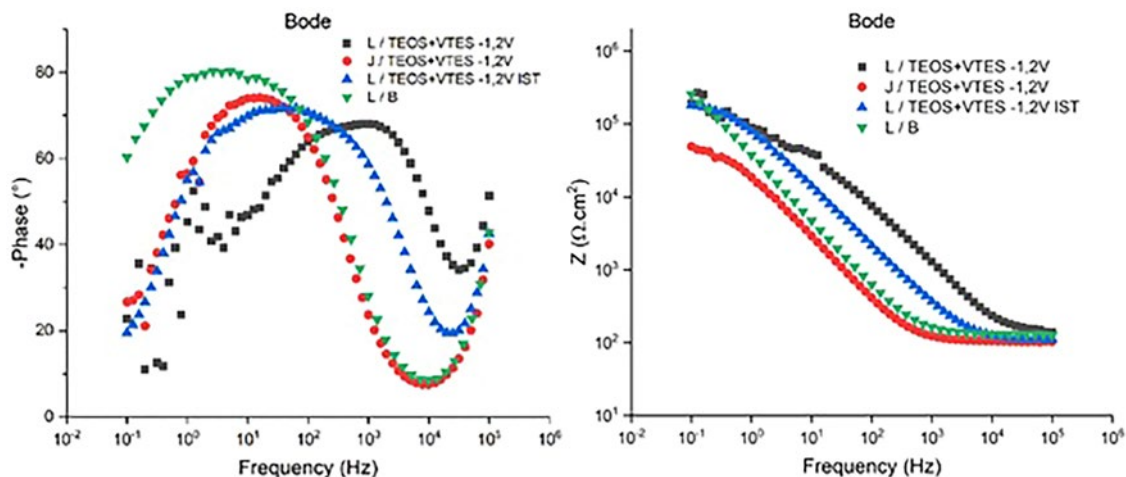


Figure 8: Bode phase diagrams plots of aluminum samples with coatings and smooth (L/VTES -1.2 V and -1.2 V IST) and sandblasted (J/VTES -1.2 V) substrates, compared to the sample without coating, L/B, after 24h of immersion in 0.1 mol/L NaCl.

relation to the others, and only with the application of the VTES coating did they show greater resistance to corrosion in the previous session. In order to minimize the pre-curing process that occurs after the deposition of TEOS NPTs, prior to this deposition, a third sample was made by mixing 50% of each solution (TEOS and VTES) using the smooth substrate and performing only the process of final curing, named L/TEOS + VTES -1.2 V IST (immersion at the same time). Figure 8 shows the Bode phase diagrams plot for the samples coated with TEOS and VTES NPTs, applying a potential of -1.2 V for the electro-assisted deposition step and comparing the result only with the L/B sample, since it has greater resistance to corrosion than the sandblasted sample due to the time constant at high to medium frequency, with a high phase angle value associated to the innermost layer of aluminum oxide, named barrier oxide. In addition, the sandblasting of the J/TEOS+VTES-1.2 V sample made its surface more active and more susceptible to corrosion.

After 24 hours of immersion, sample L/TEOS + VTES -1.2 V displayed a phenomenon at high frequency, where its curve shifted to the right, representing higher frequency values in relation to the other samples studied, which can be confirmed by summing the impedance resistances in the Bode phase diagrams plot of the phase modulus. This good performance may be associated with the efficiency of applying bisilanes (TEOS + VTES) to aluminum oxide, as the adsorption step is an important factor for the anticorrosive efficiency of silane layers. More efficient adsorption will ensure a more protective film after the film treatment (curing) steps. It is known that the number of Si-OH groups of bisilane molecules is twice that of monosilane molecules; thus, bisilanes are able to form a greater density of Me-O-Si bonds and, simultaneously, originate a more efficient polysilane film, with a greater amount of crosslinks (Si-O-Si network). A comparison of the possible interfacial regions formed between these two systems and Al is presented in Figure 9 [3], which shows in the Figure the bonds between silanes and Al substrates: (a) bis-silane; (b) monosilane. It can be observed that the interfacial region of the bis-silane/Al film (Figure 9a) has a higher density of Si-O-Si and Al-O-Si bonds than the mono-silane film (Figure 9b). As both bonds contribute to greater adhesion of silanes to the metal, bisilanes should have greater adhesion to aluminum oxide than monosilanes and, consequently, greater resistance to corrosion, as can be seen in this study, in Figure 8.

VAN SCHAFTINGHEN *et al.* [24] compared the electrochemical behavior of films with similar thicknesses of functional mono-silanes (γ -aminopropyl-triethoxy-silane, γ -APS), functional bisilanes (bis(trimethoxysilyl)propylamine, BAS) and non-functional bisilanes (bis-1,2-(triethoxysilyl)ethane, BTSE) when applied to cold-rolled steel. According to the results obtained, the best protection was conferred by BTSE, followed by BAS, while the performance of γ -APS was comparable to that of the sample not protected by the silane layer. The authors attributed their results to the formation of more cross-linked films by the bisilanes and to a possible deleterious effect of the amine group on the crosslinking. Sample L/TEOS + VTES -1.2 V IST (immersion at the same time), with only one final curing, showed a phenomenon of high to medium frequency associated with the permeability of the electrolyte through the film, denoting a performance inferior to that of sample L/TEOS + VTES -1.2 V, which was cured and immersed in 2 steps. The curing step of the coating based on alkoxide precursors must guarantee the adequate crosslinking of the film for the formation of a dense layer of

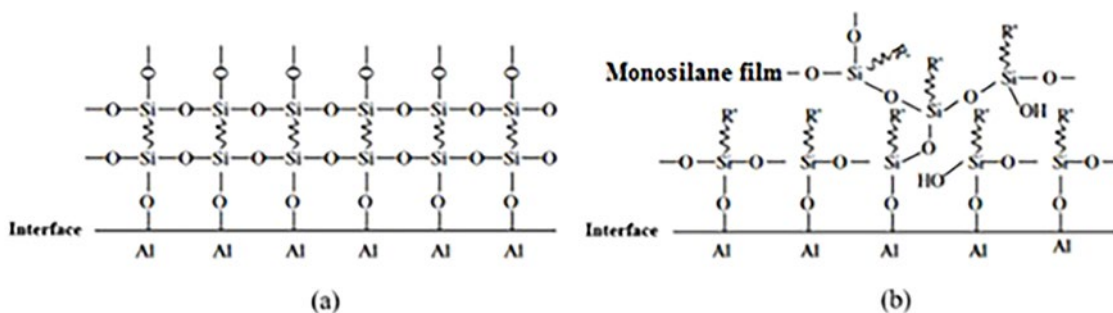


Figure 9: Bonds between silanes and Al substrates: (a) bis-silane; (b) monosilane [3].

siloxane bonds (Si-O-Si), which ensures the effectiveness of the coating since it offers protection via barrier effect [26]. Film crosslinking occurs even when the treated metal is exposed to air, albeit in a slow and incomplete manner. In view of this, studies demonstrate that the curing of the film in each immersion step induces a better and faster crosslinking of the layer [27]. The J/TEOS + VTES -1.2 V sample showed a well-defined phenomenon at medium frequency associated with the permeability of the electrolyte through the film as early as 24 hours of immersion: this behavior may be associated with the fact that there is no aluminum oxide, which, together with the silane, helps in the anticorrosive process. Results obtained by VAN OOIJ and ZHU [27] also show that silane-coated Al samples form Si-O-Si bonds during immersion in a non-corrosive electrolyte (K_2SO_4 0.5 M). The main benefit of EIS measurements of a non-corrosive electrolyte is the layer structure information that can be extracted without interference from the corrosion of the substrates. Using EIS, the authors detected, after 4 hours of immersion, an additional time constant at intermediate frequencies, which was related to a new phase formed between the aluminum oxide and the reticulated silane film (Al-O-Si) that offers better protection against corrosion. The authors observed that the additional time constant increases the impedance value even after 24 hours of immersion in the electrolyte solution. The L/B sample, on the other hand, demonstrated a “wide” phenomenon of medium to low frequency associated with corrosion products, an expected behavior since it does not have a coating and aluminum oxide is susceptible to the aggressive electrolytes of chloride ions. That is, when the passive aluminum oxide film is exposed to aggressive environments, this film is not enough to completely protect the metal, and Al and its alloys react with species in the medium, mainly chloride, to form complex interfaces. In the presence of this species, the passive film is susceptible to localized attack, which may induce the development of pitting corrosion. This form of corrosion can lead to structural attack, acting as a site for the initiation of structural cracking due to a stress corrosion mechanism [28].

Figure 10 shows the Bode phase diagrams plot for the coated samples with smooth (L/TEOS + VTES -1.2 V and -1.2 V IST) and sandblasted (J/TEOS + VTES -1.2 V) substrates, compared to the uncoated L/B sample analyzed after 48, 72 and 96 hours of immersion in 0.1 mol/L NaCl.

After 48 hours of immersion, it can be observed, with regard to the L/TEOS + VTES -1.2 V sample, that the phenomenon at high frequency associated with the barrier effect of the silane coating remains. However, there is also the appearance of a phenomenon at medium frequency associated with permeability of the electrolyte through the film, as well as a decrease in the phase angle when compared to the sample after 24 hours of immersion. After 72 and 96 hours of immersion, the phenomenon decreases at high frequency and the medium-frequency phenomenon remains, with no significant change in phase angle. Nevertheless, the only coating that maintained the phenomenon at high frequency until the end of the test was sample L/TEOS+VTES -1.2 V, which highlights the protective characteristics of this coating. CABRAL *et al.* [29] carried out a comparative study with different silanes: BTESPT, BTSE and γ -MPS, all applied to an 2024-T3 Al alloy. Analytical characterization of the silane layers was performed by Auger electron spectroscopy (AES) and X-ray photoelectron spectroscopy (XPS).

All coatings performed well against corrosion due to the decrease in corrosion speed stemming from the presence of the silane film and/or the barrier effect, which improves the protection provided by the natural oxide film. The authors compared the studied silanes using EIE and potentiodynamic polarization curves in a 0.1 M NaCl solution. All layers provided effective protection in the first hours of immersion and had a decrease in resistance at high frequency, with an increasing analysis time. Samples L/TEOS + VTES -1.2 V IST and J/TEOS+VTES -1.2 V remained with the same medium-frequency phenomenon associated with electrolyte

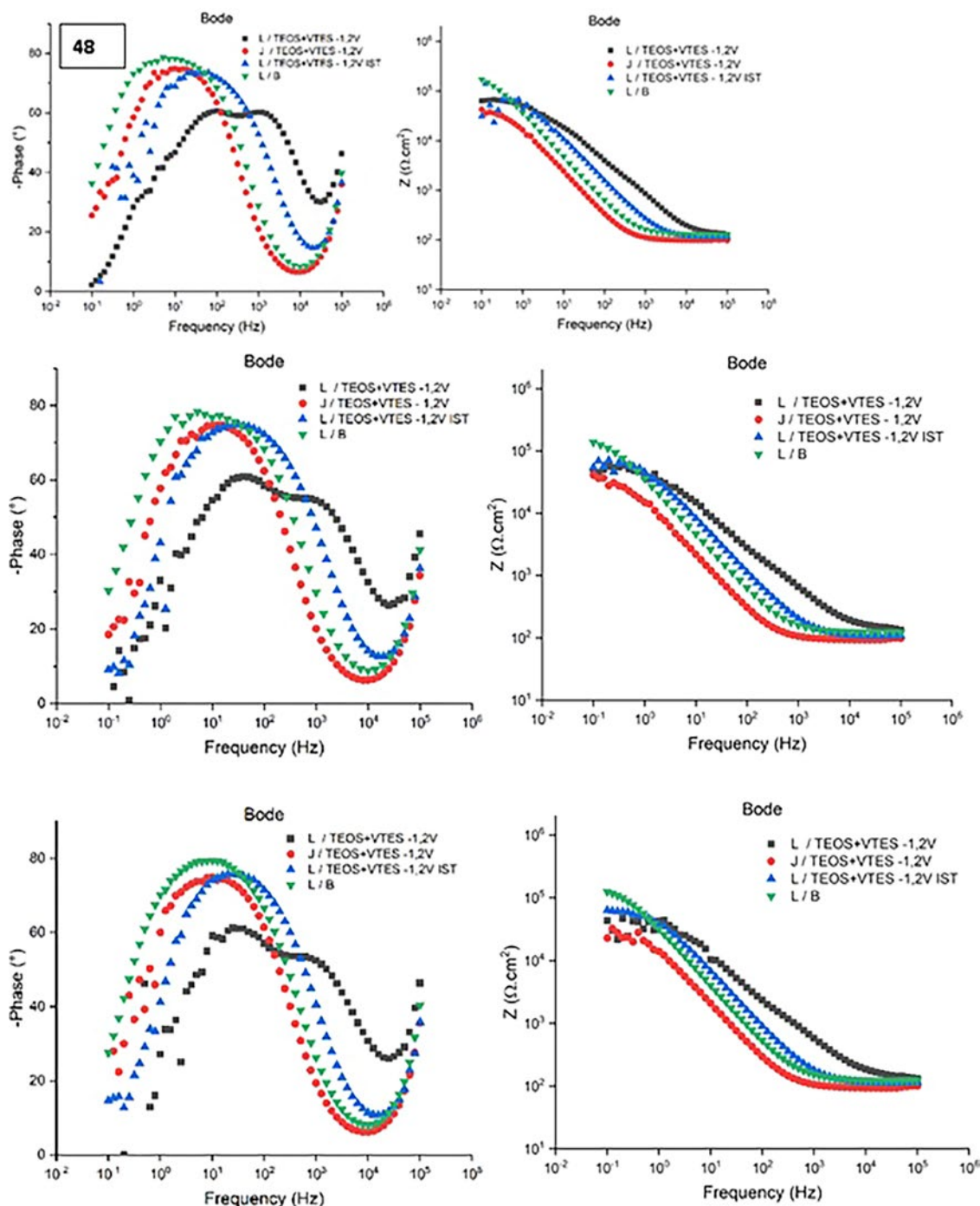


Figure 10: Bode phase diagrams plots of coated samples with smooth (L/VTES -1.2 V and -1.2 V IST) and sandblasted (J/VTES -1.2 V) substrates compared to uncoated sample L/B after 48, 72 and 96 hours of immersion in 0.1 mol/L NaCl.

permeability through the silane film and without significant difference in the phase angle value until the end of the 96-hour immersion test. In addition, these coatings showed a similarity with the uncoated sample, which also had a medium-frequency phenomenon associated with the permeability of aluminum oxide and a phase angle value slightly higher than the aforementioned coatings, denoting the fragility of the coatings as well as their low corrosive resistance. In the study by LIANG *et al.* [30], using the aluminum substrate with TEOS and VTES, the loss of superhydrophobicity was noted according to the time of immersion in solution during the EIS analysis. During this analysis, the degradation of the microstructure occurred, creating cracks in the coating – i.e., preferential pathways for the electrolytes –, with the desorption of the vinyl group also occurring due to prolonged exposure to the chloride ions. ZUCCHI and OMAR [31] used n-octadecyl-trimethoxy-silane to study

the curing of the coating by simple immersion for the formation, on copper, of a very porous, almost monomolecular interfacial layer, which was not protective. The authors performed tests using electrochemical techniques (EIS and potentiodynamic polarization curves), in addition to Fourier transform infrared spectroscopy (FTIR), to analyze a 0.6 M NaCl solution. The electrochemical tests showed that the best results were obtained by the sample cured in an oven for 1 hour at 100 °C with a two-stage immersion process, in comparison with the sample immersed with a double layer and only a final curing for 1 hour at 100°C. They also observed, via FTIR, that some silane molecules did not react between the layers in the sample that only had a final cure, resulting in a poor connection and producing an easily penetrable layer, and, consequently, compromising the anticorrosive activity of this coating [32]. The addition of TEOS NPTs to the VTES coating reduced the wettability of the samples in general, in relation to the coating containing only VTES, but the size of the nanoparticles did not supply the necessary roughness to achieve hydrophobicity (smooth) and superhydrophobicity (sandblasted) in the developed samples. Regarding all sandblasted samples, whose CA was higher than that of the smooth samples, they had low performance in terms of substrate corrosion protection, indicating some failure in the applied coating or some more hydrophilic point, which would facilitate the interaction of the substrate with the electrolyte. In the case of both coatings (VTES and NPTs + VTES), the smooth samples with a potential of -1.2 V showed better corrosion resistance properties. Furthermore, this surface, together with the bi-silane coating (TEOS NPTs + VTES), showed good resistance to corrosion at high frequencies, indicating the efficiency of the double layer of silane applied and the importance of the curing process of the coating between them.

4. CONCLUSIONS

Based on the results obtained, it can be concluded that it was possible to obtain and characterize hydrophobic coatings on the 5052 aluminum alloy using silanes, with satisfactory results in terms of substrate corrosion resistance. With regard to the VTES coating, the tests carried out verified that the potential of -1.2 V combined with the sandblasted substrate provided lower wettability. However, the electrochemical tests showed that smooth surfaces with film deposition and potentials of -1.2 V and -0.8 V had greater resistance to corrosion compared to the other analyzed samples. As to the coating with TEOS + VTES NPTs, the results demonstrated that the increase in the pH of the solution (gaining more alkalinity) influences the increase in size of the nanoparticles and that the potential of -1.2 V provides better conditions for obtaining more hydrophobic surfaces. In addition, there was a general increase in the hydrophobicity of the coated samples; that is, the presence of TEOS provided an increase in the contact angle. The electrochemical tests showed that the L/TEOS+VTES -1.2 V sample has a higher total resistance when compared to the other analyzed samples, which was associated with the efficiency of bisilanes (TEOS + VTES) on aluminum oxide. However, the IST sample, whose TEOS pre-curing process was eliminated and where both TEOS and VTES solutions were deposited simultaneously, showed worse electrochemical performance compared to the sample that had a 2-step curing. The heterogeneous surface morphology of the samples sandblasted with TEOS and/or VTES, combined with angles below 150° , decreased the corrosion resistance of these samples. Furthermore, the application of two silane coatings, as well as the two-step curing of the silanes, increased the anti-corrosion properties of the materials.

5. ACKNOWLEDGMENTS

This work was carried out with the support of CNPq, a Brazilian government entity focused on training human resources as well as encouraging science, technology and innovations. The authors also thank the financial support of Brazilian agencies: FAPERGS and CAPES.

6. BIBLIOGRAPHY

- [1] SAMANTA, A., WANG, Q., SHAW, S.K., *et al.*, "Roles of chemistry modification for laser textured metal alloys to achieve extreme surface wetting behaviors", *Materials & Design*, v. 192, n. 108, pp. 744, 2020. doi: <http://doi.org/10.1016/j.matdes.2020.108744>.
- [2] NGUYEN, T.P.N., DUFOUR, R., THOMY, V., *et al.*, "Fabrication of superhydrophobic and highly oleophobic silicon-based surfaces via electroless etching method", *Applied Surface Science*, v. 295, pp. 38–43, 2014. doi: <http://doi.org/10.1016/j.apsusc.2013.12.166>.
- [3] ZHU, D., OOIJ, W.J.V., "Corrosion protection of AA2024-T3 by bis-[3-(triethoxysilyl)propyl]tetrasulfide in sodium chloride solution. Part 2: mechanism for corrosion protection", *Corrosion Science*, v. 45, n. 10, pp. 2177–2197, 2003. doi: [https://doi.org/10.1016/S0010-938X\(03\)00061-1](https://doi.org/10.1016/S0010-938X(03)00061-1).
- [4] MITTAL, K.L., *Silanes and other coupling agents*, London, CRC Press, v. 4, pp. 421, 2007.
- [5] COSTA, J.S., *Avaliação do revestimento de conversão à base de zircônio e tanino sobre aço zincado por eletrodeposição*, Búzios, ABRACO, pp. 122, 2014.

- [6] GABBARDO, A.D., *Influência do pH e do envelhecimento da solução precursora na deposição do revestimento a base de silano BTSE com adição de inibidor Ce (III) e estudo do envelhecimento desse revestimento aplicado sobre aço galvanizado*, Fortaleza, ABRACO, pp. 98, 2014.
- [7] SILVA, R.G.C., VIEIRA, M.R.S., MALTA, M.I.C., *et al.*, “Effect of initial surface treatment on obtaining a superhydrophobic surface on 5052 aluminum alloy with enhanced anticorrosion properties”, *Surface and Coatings Technology*, v. 369, pp. 311–322, 2019. doi: <http://doi.org/10.1016/j.surfcoat.2019.04.040>.
- [8] ALIASGHARI, S., GHORBANI, M., SKELDON, P., *et al.*, “Effect of plasma electrolytic oxidation on joining of AA 5052 aluminium alloy to polypropylene using friction stir spot welding”, *Surface and Coatings Technology*, v. 313, pp. 274–281, 2017. doi: <http://doi.org/10.1016/j.surfcoat.2017.01.084>.
- [9] CABRAL, A.M., TRABELSI, W., SERRA, R., *et al.*, “The corrosion resistance of hot dip galvanised steel and AA2024-T3 pre-treated with bis-[triethoxysilylpropyl] tetrasulfide solutions doped with $Ce(NO_3)_3$ ”, *Corrosion Science*, v. 48, n. 11, pp. 3740–3758, 2006. doi: <http://doi.org/10.1016/j.corsci.2006.01.010>.
- [10] CÂNDIDO, L.C., SATHLER, L., GOMES, J.A.C.P., *Algumas considerações sobre a corrosão de Ti e Ti 6Al 4V em presença de íons fluoreto*, Rio de Janeiro, UFRJ, 2022.
- [11] RIBEIRO, D.V., SOUZA, C.A.C., ABRANTES, J.C.C., “Use of Electrochemical Impedance Spectroscopy (EIS) to monitoring the corrosion of reinforced concrete”, *RIEM - Revista IBRACON de Estruturas e Materiais*, v. 8, n. 4, pp. 529–546, 2015. <http://doi.org/10.1590/S1983-41952015000400007>.
- [12] MACDONALD, D.D., “Vacancy condensation as the precursor to passivity breakdown”, In: *Proceedings of the 12th International Corrosion Congress*, pp. 19–24, Houston, 1993.
- [13] ZHU, D., OOIJ, V.W.J., “Corrosion protection of AA 2024-T3 by bis-[3-(triethoxysilyl) propyl] tetrasulfide in neutral sodium chloride solution. Part 1: corrosion of AA 2024-T3”, *Corrosion Science*, v. 45, n. 10, pp. 2163–2175, 2003. [http://doi.org/10.1016/S0010-938X\(03\)00060-X](http://doi.org/10.1016/S0010-938X(03)00060-X).
- [14] TAMBORIM, S.M., MAISONNAVE, A.P.Z., AZAMBUJA, D.S., *et al.*, “An electrochemical and superficial assessment of the corrosion behavior of AA 2024-T3 treated with metacryloxypropylmethoxysilane and cerium nitrate”, *Surface and Coatings Technology*, v. 202, n. 24, pp. 5991–6001, 2008.
- [15] SALVADOR, D.G., MARCOLIN, P., BELTRAMI, L.V.R., *et al.*, “Development of alkoxide precursors-based hybrid coatings on Ti-6Al-4V alloy for biomedical applications: influence of pH of sol”, *Journal of Materials Engineering and Performance*, v. 27, n. 6, pp. 2863–2874, 2018. doi: <http://doi.org/10.1007/s11665-018-3368-9>.
- [16] MCCAFFERTY, E., “Sequence of steps in the pitting of aluminum by chloride ions”, *Corrosion Science*, v. 45, n. 7, pp. 1421–1438, 2003. doi: [http://doi.org/10.1016/S0010-938X\(02\)00231-7](http://doi.org/10.1016/S0010-938X(02)00231-7).
- [17] KUNST, S.R., CARDOSO, H.R.P., BELTRAMI, L.V.R., *et al.*, “New sol-gel formulations to increase the barrier effect of a protective coating against the corrosion and wear of galvanized steel”, *Materials Research*, v. 8, n. 1, pp. 138–150, 2015. doi: <https://doi.org/10.1590/1516-1439.288914>.
- [18] TEO, M., KIM, J., WONG, P.C., *et al.*, “Investigations of interfaces formed between bis-1,2-(triethoxysilyl)ethane (BTSE) and aluminum after different Forest Product Laboratory pre-treatment times”, *Applied Surface Science*, v. 221, n. 11–14, pp. 340–348, 2004. [http://doi.org/10.1016/S0169-4332\(03\)00933-4](http://doi.org/10.1016/S0169-4332(03)00933-4).
- [19] BRINKER, C.J., SCHERER, G.W., “Drying”, In: Brinker, C.J., Scherer, G.W., *Sol-Gel Science: The Physics and Chemistry of Sol-Gel Processing*, USA, Elsevier, pp. 452–513, 1990. doi: <http://doi.org/10.1016/B978-0-08-057103-4.50013-1>.
- [20] SALVADOR, D.G., MARCOLIN, P., BELTRAMI, L.V.R., *et al.*, “Influence of the pretreatment and curing of alkoxysilanes on the protection of the titanium-aluminum-vanadium alloy”, *Journal of Applied Polymer Science*, v. 134, n. 46, pp. 45470, 2017. doi: <http://doi.org/10.1002/app.45470>.
- [21] BAUER, D.R., MARTIN, J.W., *Service life prediction of organic coatings: a systems approach*, Washington: American Chemical Society, v. 722, 1999. doi: <http://doi.org/10.1021/bk-1999-0722>.
- [22] RAHIMI, H., MOZAFFARINIA, R., NAJAFABADI, A.H., “Corrosion and wear resistance characterization of environmentally friendly sol-gel hybrid nanocomposite coating on AA5083”, *Journal of Materials Science and Technology*, v. 29, n. 7, pp. 603–608, 2013. doi: <http://doi.org/10.1016/j.jmst.2013.03.013>.
- [23] BERENDSEN, C.W.J., ŠKERENJ, M., NAJDEK, D., *et al.*, “Superhydrophobic surface structures in thermoplastic polymers by interference lithography and thermal imprinting”, *Applied Surface Science*, v. 255, n. 23, pp. 9305–9310, 2009. doi: <http://doi.org/10.1016/j.apsusc.2009.07.001>.
- [24] VAN SCHAFTINGHEN, T., LE PEN, C., TERRY, H., *et al.*, “Investigation of the barrier properties of silanes on cold rolled steel”, *Electrochimica Acta*, v. 49, n. 17–18, pp. 2997–3004, 2004.

- [25] MENEZES, T.L., *Revestimentos a base de silanos nanoestruturados para a proteção contra a corrosão em aço galvanizado*, Porto Alegre, Editora da UFRGS, pp. 179, 2015.
- [26] PALOMINO, L.E.M., CASTRO, J.F.W., AOKI, I.V., *et al.*, “Microstructural and electrochemical characterization of environmentally friendly conversion layers on aluminium alloys”, *Journal of the Brazilian Chemical Society*, v. 14, n. 4, pp. 651–659, 2003. doi: <http://doi.org/10.1590/S0103-50532003000400024>.
- [27] VAN OOIJ, W.J., ZHU, D., “Electrochemical impedance spectroscopy of Bis [Triethoxysilylpropyl] tetrasulfide on Al 2024-T3 substrates”, *Corrosion*, v. 57, n. 5, pp. 413–427, 2001. doi: <http://doi.org/10.5006/1.3290365>.
- [28] FALAVIGNA, G.S., KUNST, S.R., FERREIRA, J.Z., *et al.*, “Influência do Nb contido em eletrólito a base de oxalato na anodização de alumínio em ácido oxálico”, *Research Society and Development*, v. 10, n. 12, pp. e226101220369, 2021. doi: <http://doi.org/10.33448/rsd-v10i12.20369>.
- [29] CABRAL, A.M., DUARTE, R.G., MONTEMOR, M.F., *et al.*, “A comparative study on the corrosion resistance of AA2024-T3 substrates pre-treated with different silane solutions”, *Progress in Organic Coatings*, v. 54, n. 4, pp. 322–331, 2005. doi: <http://doi.org/10.1016/j.porgcoat.2005.08.001>.
- [30] LIANG, J., HU, Y., WU, Y., *et al.*, “Facile formation of superhydrophobic silica-based surface on aluminum substrate with tetraethylorthosilicate and vinyltriethoxysilane as co-precursor and its corrosion resistant performance in corrosive NaCl aqueous solution”, *Surface and Coatings Technology*, v. 240, pp. 145–153, 2014. doi: <http://doi.org/10.1016/j.surfcoat.2013.12.028>.
- [31] ZUCCHI, F., OMAR, I.H., “Plant extracts as corrosion inhibitors of mild steel in HCl solutions”, *Surface Technology*, v. 24, n. 4, pp. 391–399, 1985. doi: [http://doi.org/10.1016/0376-4583\(85\)90057-3](http://doi.org/10.1016/0376-4583(85)90057-3).
- [32] SUERO, D.L., ROMO, F.J.C., CRUZ, M.D., *et al.*, “Optimizing copper anticorrosive protection: properties of GPTMS-TiO₂ hybrid organic-inorganic sol-gel coatings via the dip-coating technique”, *Revista Matéria*, v. 24, n. 4, pp. e20240169, 2024. doi: <https://doi.org/10.1590/1517-7076-RMAT-2024-0169>.